



# Self-consistent hydrodynamic solutions for line-driven winds of O stars in the m-CAK formalism

A.C. Gormaz-Matamala<sup>1,2</sup>, M. Curé<sup>1,2</sup>, L.S. Cidale<sup>3,4</sup> & R.O.J. Venero<sup>3,4</sup>

<sup>1</sup> *Instituto de Física y Astronomía, Universidad de Valparaíso, Valparaíso, Chile*

<sup>2</sup> *Centro de Astrofísica, Universidad de Valparaíso, Valparaíso, Chile*

<sup>3</sup> *Departamento de Espectroscopía, Facultad de Ciencias Astronómicas y Geofísicas, UNLP, Argentina*

<sup>4</sup> *Instituto de Astrofísica de La Plata, CONICET-UNLP, Argentina*

Contact / alex.gormaz@postgrado.uv.cl

**Resumen** / El viento de las estrellas masivas está impulsado principalmente por la transferencia de momento del campo de radiación a la atmósfera estelar, mediante una enorme cantidad de líneas espectrales (teoría m-CAK). En este trabajo, presentamos los resultados de un procedimiento autoconsistente para obtener la solución hidrodinámica del viento (campo de velocidades y tasa de pérdida de masa) conjuntamente con los parámetros de la fuerza de radiación en líneas, considerando la contribución de más de 900,000 transiciones. Los modelos fueron calculados para estrellas con temperaturas efectivas mayores a 32,000 K y gravedades superficiales mayores a 3.4 dex, considerando además diferentes metalicidades. Comparamos los perfiles de línea sintéticos calculados a partir de nuestras soluciones hidrodinámicas usando el código FASTWIND, con espectros observados de estrellas O. Demostramos que los resultados de nuestro procedimiento se encuentran en buen acuerdo con las observaciones, cuando se tienen en cuenta los factores de *clumping* apropiados.

**Abstract** / The wind of massive stars is driven mainly by the transfer of momentum from the radiation field, to the stellar atmosphere through a large number of line transitions (m-CAK theory). In this work, we present some of the results of a self-consistent procedure to calculate the wind hydrodynamic solution (velocity field and mass-loss rate) along with the line-force parameters, considering the contribution of more than 900,000 line transitions. The models were computed for stars with effective temperatures above 32,000 K and surface gravities higher than 3.4 dex, also considering different metallicities. We compare the synthetic line profiles obtained from our hydrodynamic solutions using the code FASTWIND, with observed O stellar spectra. We show that the computed line profiles fits quite well the observations when appropriate clumping factors are taken into account.

*Keywords* / hydrodynamics — methods: analytical — stars: early-type — stars: mass-loss — stars: winds, outflows

## 1. Theoretical background

According to Castor et al. (1975), for massive stars, the line-acceleration is given by:

$$g_{\text{line}} = \frac{\sigma_e L_*}{4\pi r^2 c} \mathcal{M}(t), \quad (1)$$

where  $\mathcal{M}(t)$  is the so-called line-force multiplier factor;  $L_*$  is the stellar luminosity;  $r$  is the distance;  $c$  is the speed of light; and  $\sigma_e$  is the Thomson scattering opacity.

$\mathcal{M}(t)$  is expressed in terms of the modified optical depth  $t$  which depends on the density  $\rho$ , the thermal velocity  $v_{\text{th}}$  and the velocity gradient:

$$t = \sigma_e \rho(r) v_{\text{th}} \left( \frac{dv}{dr} \right)^{-1}. \quad (2)$$

Abbott (1982) parametrized the line-force multiplier as:

$$\mathcal{M}(t) = k t^{-\alpha} \left( 10^{-11} \frac{N_e}{W} \right)^\delta. \quad (3)$$

with  $N_e$ , the electron density and  $W(r)$ , the dilution factor. The parameters  $k$ ,  $\alpha$ , and  $\delta$  are called line-force [multiplier] parameters.

In this article, we present some of the results obtained by (Gormaz-Matamala et al., 2019) through a self-consistent prescription that includes the calculation of the line-force parameters, for a wide range of stellar parameters. Line-force parameters are calculated considering the contribution of hundreds of thousands of lines involved in the absorption and reemission processes, a quasi-NLTE approach for the ionic populations, together with the hydrodynamics provided by the code HYDWIND (Curé, 2004), in an iterative procedure. The models were computed for stars with effective temperatures above 32,000 K and surface gravities higher than 3.4 dex, considering also different metallicities. Using the atmosphere code FASTWIND, we compute the synthetic line profiles resulting from our hydrodynamic solutions and compare them with observed O star spectra.

## 2. Results

The computed line-force parameters ( $k, \alpha, \delta$ ) show a clear trend with the effective temperature  $T_{\text{eff}}$  (in kK), the surface gravities  $\log g$  and metallicities, as it is shown in Figure 1.

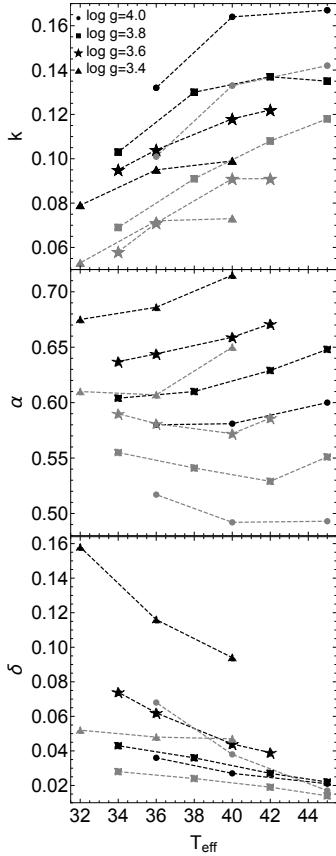


Figure 1: The line-force parameters as a function of  $T_{\text{eff}}$ , for different values of  $\log g$ . Black dashed lines correspond to models with solar metallicity and grey dashed lines, for  $Z = Z_{\odot}/5$ .

Our self-consistent solutions (Figure 2, upper panels) produce a more clear behaviour for the changes of the wind parameters with effective temperature and  $\log g$ , than those obtained from the Abbott’s line-force parameters (Abbott, 1982, lower panels).

With respect to terminal velocities, we observe that  $\alpha$  values present a wide dispersion, in contrast with the linear relationship found by Puls et al. (2008):

$$v_{\infty} \approx 2.25 \sqrt{\frac{\alpha}{1-\alpha}} v_{\text{esc}}. \quad (4)$$

Figure 3 shows a different linear behaviour than Equation 4, that strongly depends on the value of  $\log g$ .

Comparison of mass-loss rates (upper panel) and terminal velocities (lower panel) as a function of the effective temperature it is shown in Figure 4. Blue stars correspond to results from this work, black disks to Bouret et al. (2005) and Markova et al. (2018) results, and red triangles to theoretical values from Vink et al. (2001). The same colour code but with modified symbols (inverted blue stars, unfilled black circles and inverted red triangles) are used to represent Markova’s stars with the same effective temperature but higher surface gravity.

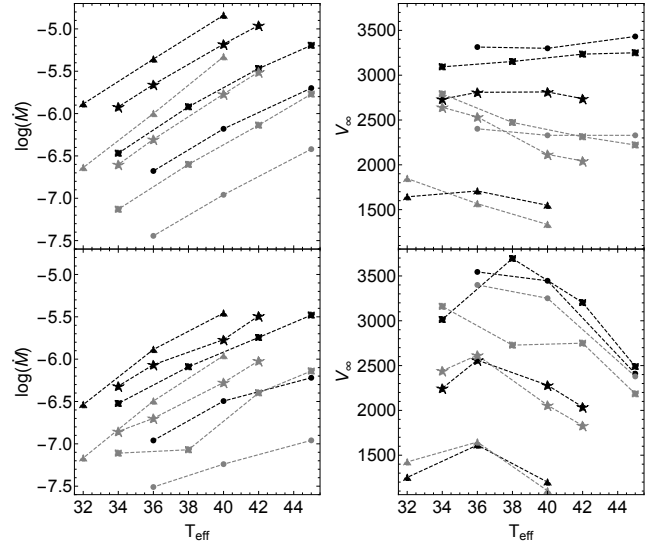


Figure 2: Behavior of  $\dot{M}$  and  $v_{\infty}$  as a function of  $T_{\text{eff}}$  (in kK) for different abundances and gravities. Top panels are for self-consistent calculations and bottom panels are for Abbott’s procedure. Symbol description is the same as that in Figure 1.

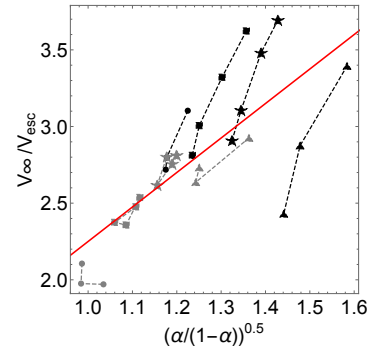


Figure 3:  $v_{\infty}/v_{\text{esc}}$  versus  $\sqrt{\alpha/(1-\alpha)}$ . For each set of  $\log g$  values there is a linear dependence for  $Z_{\odot}$ . Slope 2.25 of Equation 4 (red line) is also displayed. For sub-solar abundance there is a unique linear relationship.

### 3. Synthetic spectra

The resulting spectra, obtained with FASTWIND and fitted to the observed one for the star  $\zeta$ -Puppis, is shown in Figure 5. The model was computed with  $T_{\text{eff}} = 40$  kK,  $\log g = 3.64$ ,  $R_*/R_{\odot} = 18.6$  and  $\dot{M} = 5.2 \times 10^{-6} M_{\odot} \text{yr}^{-1}$ . Clumping factors are  $f_{\text{cl}} = 1.0$  (red, homogeneous),  $f_{\text{cl}} = 5.0$  (blue) and  $f_{\text{cl}} = 9.0$  (green):

This plot clearly shows that self-consistent line-force and wind parameters leads to a good solution, producing a synthetic spectrum. The only free parameter here is the clumping factor, which is set to adjust the shape of  $\text{H}\alpha$ .

### 4. Conclusions

In the present work we have presented some of the results of our procedure to calculate self-consistent, line-force parameters coupled with the hydrodynamics, in

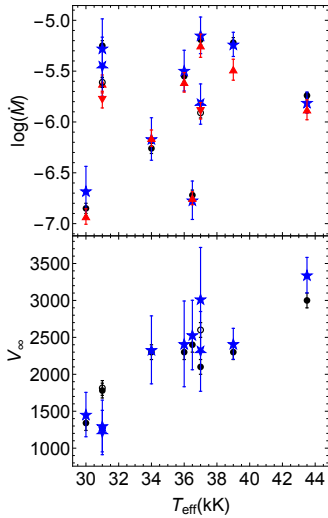


Figure 4: Comparison of mass-loss rates and terminal velocities as a function of the effective temperature obtained by different authors. The references of the symbols are in the text.

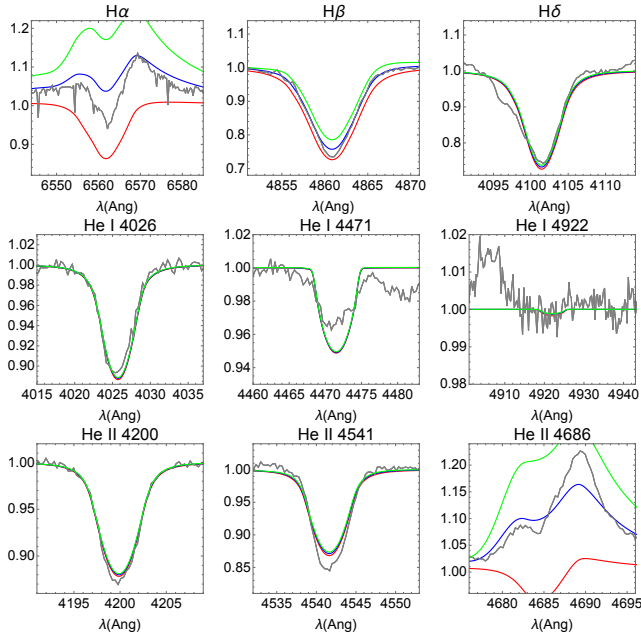


Figure 5: Line profile fits (normalized fluxes) for the spectra of  $\zeta$ -Puppis. The color code is in the text.

the frame of the radiation driven wind theory. Thanks to this procedure we achieve a unique, well-converged solution that does not depend on the chosen initial values. This is important because it reduces the number of free parameters (now  $\beta$ , the power of the  $\beta$ -velocity law,  $v_\infty$  and  $\dot{M}$  are no more input parameters) to be determined by fitting synthetic spectra to observed ones.

The set of solutions differs from previous line-force parameter calculations performed by Abbott (1982) and Noebauer & Sim (2015). With these new values, we

found a different scale relation for the terminal velocity that is steeper than the usually accepted one. This new relation might explain the observed scatter found in the terminal velocity from massive stars located at the hot side of the bistability jump (Markova & Puls, 2008).

Concerning the wind parameters derived from modelling O-type stars with homogeneous winds, our mass-loss rates are in better agreement with the predicted ones given by Vink et al. (2001) formula.

For the calculation of synthetic spectra for  $\zeta$ -Puppis, we conclude that our procedure's values for mass-loss rate and hydrodynamics reproduce the observed line profiles when an adequate value for the clumping factor is chosen.

Even knowing the limitations of the m-CAK theory, this remains an extremely useful framework to get an estimate of the real parameters of stellar winds on massive stars. In spite of the approximations assumed under this theory, we obtain reliable values for mass-loss rates and self-consistent hydrodynamics in a short period of time with great CPU time savings.

Our new self-consistent procedure can be used to derive accurate mass-loss rates and: (i) study evolutionary tracks, where a high precision on terminal velocities is not required, and (ii) derive trusty clumping factors via line-profile fittings.

*Acknowledgements:* We sincerely thank J. Puls for helpful discussions that improved this work and for having put to our disposal his code FASTWIND. We are very grateful to D. J. Hillier for allowing us to use CMFGEN-atomic-data and providing us with the observed spectrum of  $\zeta$ -Puppis. A.C.G.M. has been financially supported by the PhD Scholarship folio N° 2116 1426 from National Commission for Scientific and Technological Research of Chile (CONICYT). A.C.G.M. is also thankful for support from the Chilean Astronomical Society (SOCHIAS). A.C.G.M. and M.C. acknowledge support from Centro de Astrofísica de Valparaíso. M.C. and L.S.C. are thankful for support from the project CONICYT+PAI/Atracción de Capital Humano Avanzado del Extranjero (Folio PAI80160057). M.C. thanks the support from FONDECYT project 1190485. L.S.C. and R.O.J.V. acknowledges financial support from the Universidad Nacional de La Plata (Programa de Incentivos G11/137), the CONICET (PIP 0177), and the Agencia Nacional de Promoción Científica y Tecnológica (Préstamo BID, PICT 2016/1971), Argentina. This project has received funding from the European Union's Framework Programme for Research and Innovation Horizon 2020 (2014-2020) under the Marie Skłodowska-Curie grant Agreement No. 823734.

## References

- Abbott D.C., 1982, ApJ, 259, 282  
 Bouret J.C., Lanz T., Hillier D.J., 2005, A&A, 438, 301  
 Castor J.I., Abbott D.C., Klein R.I., 1975, ApJ, 195, 157  
 Curé M., 2004, ApJ, 614, 929  
 Gormaz-Matamala A.C., et al., 2019, ApJ, 873, 131  
 Markova N., Puls J., 2008, A&A, 478, 823  
 Markova N., Puls J., Langer N., 2018, A&A, 613, A12  
 Noebauer U.M., Sim S.A., 2015, MNRAS, 453, 3120  
 Puls J., Vink J.S., Najarro F., 2008, A&A Rv, 16, 209  
 Vink J.S., de Koter A., Lamers H.J.G.L.M., 2001, A&A, 369, 574